A Comparative Fully Relativistic/Nonrelativistic First-Principles Xα–DVM and Photoelectron Spectroscopic Investigation of Electronic Structure in Homologous 4f and 5f Tris(η^5-cyclopentadienyl)metal(IV) Alkoxide Complexes†,‡

Antonino Gulino, Santo Di Bella, and Ignazio Fragalà*

Dipartimento di Scienze Chimiche, Univeristà di Catania, Viale Andrea Doria 8, 95125 Catania, Italy

Maurizio Casarin

Dipartimento di Chimica Inorganica, Metallorganica ed Analitica, Università di Padova, 35100 Padova, Italy

Afif M. Seyam§ and Tobin J. Marks*

Department of Chemistry, Northwestern University, Evanston, Illinois 60208-3113

Received February 8, 1993

The electronic structure of $(\eta^5\text{-}C_5H_5)_3MOR$ (M = Ce, Th, U) complexes has been investigated by He I and He II UV photoelectron spectroscopy combined with SCF Xα–DVM calculations. Fully relativistic Dirac–Slater calculations were also carried out for the M = Th complex. The nonrelativistic calculations indicate that metal–ligand interactions involving the highest energy ligand orbitals involve primarily metal 5f orbitals while 6d admixtures are found for lower energy orbitals. The M–O bonding is both σ and π in nature and involves primarily metal 6d atomic orbitals. Evidence of a charge redistribution mechanism along the $CH_3\rightarrow O\rightarrow M\rightarrow Cp_3$ direction provides a satisfactory explanation for the shortened M–O distances and strong propensity for nearly linear M–O–CH_3 linkages observed in diffraction studies. The fully relativistic calculations show that metal d contributions are slightly underestimated at the nonrelativistic level. Such deviations do not, however, alter the overall description of the metal–ligand bonding. The nonrelativistic configuration of the metal center compares well with the relativistic data. Gas-phase ionization energies can be accurately and comparably evaluated at the computationally more efficient nonrelativistic level if optimized basis sets and potential representations are used.

Introduction

The electronic structure of f-element organometallic molecules has been the subject of recent active investigation. Valuable information has emerged from experimental photoelectron spectroscopic studies[1] as well as from purely theoretical investigations.[2] Contributions have reported on various classes of f-element complexes, and different theoretical formalisms have invariably yielded similar bonding pictures. In particular, it has been demonstrated that both 5f and 6d AOs are important for actinide–ligand bonding,[3] even though the neglect of relativistic corrections results in some over- and underestimation of covalent mixing involving 5f and 6d metal orbitals, respectively. When lanthanides are considered, the situation appears somewhat less certain. According to conventional chemical wisdom, the 4f electrons act as simple spectators in the chemical bonding.[4] There is, however, experimental evidence that these subshells may affect both the bonding[5] as well as related physicochemical parameters.[6]

In principle, comparative electronic structure studies of a homologous series of 4f and 5f complexes can provide considerable insight into orbital participation issues. Of the two existing series of homologous organolanthanide/organoactinide complexes, only the $M(\eta^8\text{-}C_8H_8)_2$ series (M = Ce, Th, U) has been analyzed in depth.[7] For the Cp_3MOR series (Cp = $\eta^5\text{-}C_5H_5$, M = Ce, Th, U), which offers the possibility of comparing and contrasting both 4f/5f metal–ligand σ and π bonding, only the electronic structure of the M = Ce congener has been studied in detail.[8] As a part of our ongoing experimental and theoretical electronic structure studies of a wide variety of classical[9] and organometallic[1,3,10] f-element complexes, we now report a comparative electronic structure study of the Cp_3MOR alkoxides of Th(IV), U(IV), and Ce(IV). The present contribution includes a *fully relativistic*

† Photoelectron Spectroscopy of f-Element Organometallic Complexes. 9. For part 8 see ref 1a.

‡ Abstracted in part from the Ph.D. thesis of A.G., Università di Catania, 1989.

§ On leave from the Department of Chemistry, University of Jordon, Amman, Jordan.

(1) (a) Gulino, A.; Ciliberto, E.; Di Bella, S.; Fragalà, I.; Seyam, A. M.; Marks, T. J. *Organometallic* **1992**, *11*, 3248–3257 and references therein. (b) Burns, C. J.; Bursten, B. E. *Comments Inorg. Chem.* **1989**, *2*, 61–93. (c) Arduini, A. L.; Malito, J.; Takats, J.; Ciliberto, E.; Fragalà, I.; Zanella, P. *J. Organomet. Chem.* **1987**, *326*, 49–58 and references therein. (d) *Fundamental and Technological Aspects of Organo-f-Element Chemistry;* Marks, T. J., Fragalà, I. L., Eds.; D. Reidel Publishing Co.: Dordrecht, Holland, 1985. (e) Fragalà, I. In *Organometallics of the f-Elements*; Marks, T. J., Fischer, R. D., Eds.; Reidel Publishing Co.: Dordrecht, Holland, 1979; pp 421–466.

(2) For excellent reviews see: (a) Bursten, B. E.; Strittmatter, R. J. *Angew. Chem., Int. Ed. Engl.* **1991**, *30*, 1069–1085. (b) Pepper, M.; Bursten, B. E. *Chem. Rev.* **1991**, *91*, 719–741. (c) Pyykkö, P. *Chem. Rev.* **1988**, *88*, 563–594. (d) Pyykkö, P. *Inorg. Chim. Acta* **1987**, *139*, 243–245.

(3) (a) Bursten, B. E.; Rhodes, L. F.; Strittmatter, R. J. *J. Am. Chem. Soc.* **1989**, *111*, 2758–2766. (b) Vittadini, A.; Casarin, M.; Ajò, D.; Bertoncello, R.; Ciliberto, E.; Gulino, A.; Fragalà, I. *Inorg. Chim. Acta* **1986**, *121*, L23–L25. (c) Fragalà, I.; Ciliberto, E.; Fischer, R. D.; Sienel, G.; Zanella, P. *J. Organomet. Chem.* **1976**, *120*, C9–C12.

(4) Lohr, L. L.; Jia, Y. Q. *Inorg. Chim. Acta* **1986**, *119*, 99–105.

(5) Ruscic, B.; Goodman, G. L.; Berkowitz, J. *J. Chem. Phys.* **1983**, *78*, 5443–5467.

(6) (a) Murad, E.; Hildenbrand, D. L. *J. Chem. Phys.* **1980**, *73*, 4005. (b) Ames, L. L.; Walsh, P. N.; White, D. *J. Phys. Chem.* **1967**, *71*, 2707.

(7) (a) Chang, A. H. H.; Pitzer, R. M. *J. Am. Chem. Soc.* **1989**, *111*, 2500–2507. (b) Rösch, N. *Inorg. Chim. Acta* **1984**, *94*, 297–299.

(8) Gulino, A.; Casarin, M.; Conticello, V. P.; Gaudiello, J. G.; Mauermann, H.; Fragalà, I.; Marks, T. J. *Organometallics* **1988**, *7*, 2360.

(9) (a) Bursten, B. E.; Casarin, M.; Ellis, D. E.; Fragalà, I.; Marks, T. J. *Inorg. Chem.* **1986**, *25*, 1257–1261. (b) Fragalà, I.; Condorelli, G.; Tondello, E.; Cassol, A. *Inorg. Chem.* **1978**, *17*, 3175.

0020-1669/93/1332-3873$04.00/0

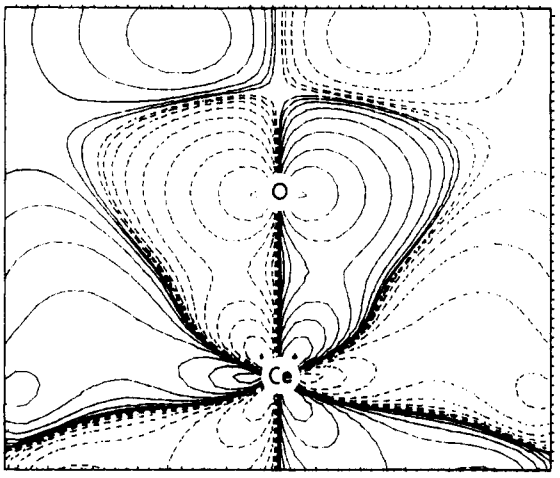

Figure 1. DV–Xα contour plot of the 20a″ MO (HOMO) in the *yz* plane for the Cp_3CeOCH_3 molecule. The contour values are ±0.0065, ±0.013, ±0.026, ±0.052, ±0.104, ±0.208, ±0.416, and ±0.832 $e^{1/2}$ Å$^{3/2}$. Dashed lines refer to negative values.

Chart I

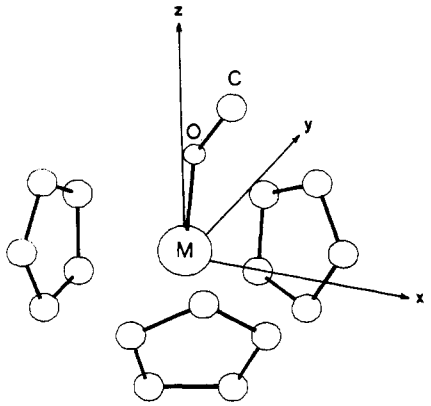

local density Xα–DV calculation on the Th(IV) complex and nonrelativistic Xα–DV treatments of all the complexes. Gas-phase He I and He II photoelectron spectroscopic data are also reported and correlated with the theoretical results.

There is evidence that inclusion of relativistic effects is particularly critical for calculations on Th complexes since the differential energy destabilization of *nf* and $(n + 1)$d AOs results in an inverted f and d orbital sequence in the Th atom.[11] In contrast, for U and Ce, the f orbitals remain lower in energy than d orbitals.[5,11] For this reason, relativistic calculations on Cp_3ThOR have been used to further test the reliability of the nonrelativistic approach, since previous studies[1] have suggested that the overall description of the metal–ligand bonding is comparable in both relativistic and nonrelativistic cases and have raised doubts as to whether an admittedly more rigorous relativistic evaluation of 5f vs 6d admixtures is worth the prodigious computational effort.

Experimental Section

The Cp_3MOR complexes studied (M = Ce, R = *i*-Pr; M = Th, R = CH_3; M = U, R = C_2H_5) were selected because of their volatility and high thermal stability. They were synthesized according to published procedures[8,12] and were purified by sublimation in vacuo. The compounds were always handled under a prepurified argon atmosphere and gave satisfactory analytical results. High-resolution UV photoelectron (PE) spectra were recorded in the 120–140 °C temperature range, depending upon the particular complex. Spectra were accumulated with an IBM AT computer directly interfaced to the PE spectrometer, which was equipped with a He I, He II source (Helectros Development). Resolution measured on the Ar $^2P_{3/2}$ line was always around 20–25 meV. He II spectra were corrected only for the He IIβ "satellite" contributions (9% on the reference N_2 spectrum). The spectra were deconvoluted by fitting the spectral profiles with a series of asymmetrical Gaussian envelopes after subtraction of the background. The asymmetric Gaussian peaks are defined by the peak position, the amplitude, and the half-widths (W_L, W_R). The agreement factors, $R = [\sum(F_o - F_c)^2/\sum(F_o)^2]^{1/2}$, after minimization of the function $\sum(F_o - F_c)^2$ converged to values ≤0.036. The band areas thus evaluated were corrected for the analyzer transmission function.

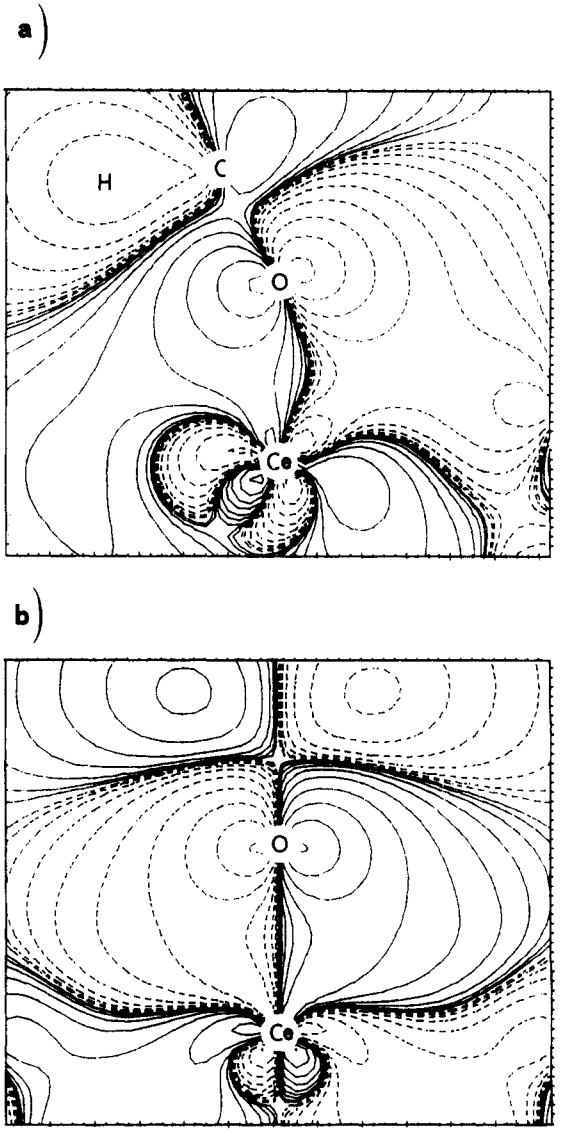

Figure 2. DV–Xα contour plots of the (a) 24a′ and (b) 17a″ MOs in the *xz* and *yz* planes, respectively, for the Cp_3CeOCH_3 molecule. The contour values are ±0.0065, ±0.013, ±0.026, ±0.052, ±0.104, ±0.208, ±0.416, and ±0.832 $e^{1/2}$ Å$^{3/2}$. Dashed lines refer to negative values.

Computational Details

Nonrelativistic quantum mechanical calculations were carried out within the DV–Xα formalism.[13] The molecular electron density was

(10) (a) Fragalà, I.; Gulino, A. In ref 1d, pp 327–360. (b) Bruno, G.; Ciliberto, E.; Fischer, R. D.; Fragalà, I.; Spiegl, A. W. *Organometallics* **1983**, *2*, 1060–1062. (c) Green, J. C.; Payne, M. P.; Streitwieser, A., Jr. *Organometallics* **1983**, *2*, 1707–1710. (d) Ciliberto, E.; Condorelli, G.; Fagan, P. J.; Manriquez, J. M.; Fragalà, I.; Marks, T. J. *J. Am. Chem. Soc.* **1981**, *103*, 4755–4759. (e) Fragalà, I.; Condorelli, G.; Zanella, P.; Tondello, E. *J. Organomet. Chem.* **1976**, *122*, 357–363.

(11) Pyykkö, P.; Laakkonen, L. J.; Tatsumi, K. *Inorg. Chem.* **1989**, *28*, 1801.

(12) Marks, T. J.; Ernst, R. D. In *Comprehensive Organometallic Chemistry*; Wilkinson, G., Stone, F. G. A., Abel, E. W., Eds.; Pergamon Press: Oxford, U.K., 1982; Chapter 21 and references therein.

(13) (a) Averill, F. W.; Ellis, D. E. *J. Chem. Phys.* **1973**, *59*, 6411–6418. (b) Rosen, A.; Ellis, D. E.; Adachi, H.; Averill, F. W. *J. Chem. Phys.* **1976**, *65*, 3629–3634 and references therein. (c) Trogler, W. C.; Ellis, D. E.; Berkowitz, J. *J. Am. Chem. Soc.* **1979**, *101*, 5896–5901. (d) Ellis, D. E. In *Actinides in Perspective*; Edelstein, N. M., Ed.; Pergamon Press: Oxford, U.K., 1982; pp 123–143.

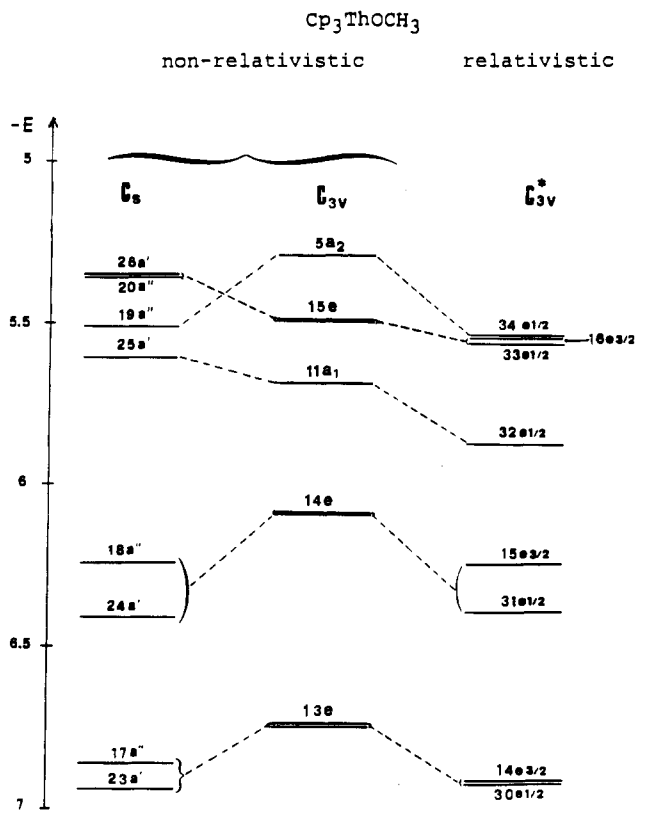

Figure 3. Correlation diagram for the uppermost MOs of Cp_3ThOCH_3 obtained from nonrelativistic (C_s and C_{3v}) and relativistic C_{3v}* ground-state calculations.

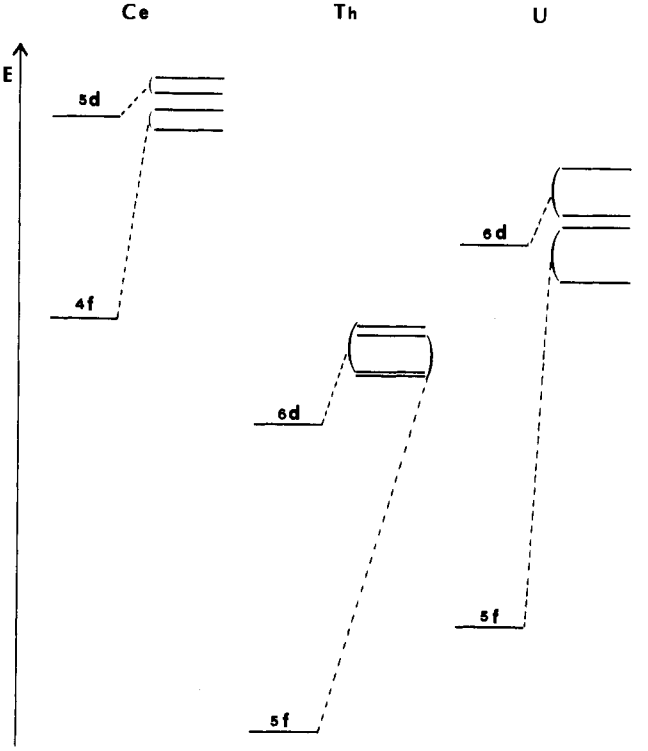

Figure 4. Comparison between relativistic and nonrelativistic energies of nf and $(n+1)$d AOs of the Ce, Th, and U bare ions (see Computational Details in the text).

approximated with an s-wave expansion to evaluate the Coulomb potential. The SCF equations were converged using a self-consistent charge (SCC) procedure.[13] Since earlier studies[1a] on similar complexes have shown that the inclusion of multipolar fitting functions to describe the charge density does not consistently improve the final results, numerical AOs (atomic orbitals) (through 7p on Th and U, 6p on Ce, 2p on O and C, and 1s on H) were used as basis functions.[13] Several numerical calculations have been carried out in order to find the best basis set.[14] The integration mesh used 2400 points around the U and Th atoms, 1200 points around Ce atom, 150 points around C and O atoms, and finally 75 points around H atoms. A total of 5100–6300 sample points were used. A frozen core approximation (1s...6p on Th, U; 1s...5p on Ce; 1s on O and C) was used throughout the calculations.[13] The ionization energies (IEs) were evaluated within the Slater transition state formalism (TSIEs)[15] to account for reorganization effects upon ionization. Contour plots (CPs) of some selected molecular orbitals (MOs) have been also analyzed.

The fully relativistic molecular calculations on Cp_3ThOCH_3 were performed using the local density Dirac–Slater (DS) formalism[16] which accommodates both spin and orbital operators. The solution of the time-independent single-electron Dirac equation[16d]

$$h = c\alpha[p - (e/c)A] + mc^2\beta + eA_0$$

intrinsically leads to four-component wave functions Φ_n. The exchange parameter α was set to a uniform value of 0.7 in all calculations. To localize the more diffuse valence states, a potential well of depth −2.0 au with an inner radius of 4.0 au and an outer radius of 6.0 au was added to the atomic potential. The functions were sampled to 11 917 points. A basis set also including the 6s and 6p functions was used for the Th atom.

Model Cp_3MOCH_3 structures, simplified to C_s symmetry, were used throughout the calculations. In the relativistic calculation, the model was further idealized to C_{3v} symmetry with a linear Th–O–CH_3 vector in order to decrease the required computational demands. In all calculations, the geometry of the MCp_3 cluster was frozen with a 117° Cp(centroid)–M–Cp(centroid) angle and a 2.54 Å M–Cp(centroid) distance in accord with experiment.[17] The M–O–CH_3 angle was taken to be 154°, and 180° in the nonrelativistic calculations (results for both geometries were essentially identical), and the M–O distances were extrapolated from data on suitable related complexes.[9,17]

The influence of relativistic effects on the energies of the valence AOs of the bare Ce, Th, and U ions was checked by suitable relativistic calculations where the relevant AO energies were optimized, starting from the nonrelativistic electronic configurations found in the present complexes. Nonrelativistic calculations were run on a Vax-11/750 minicomputer. DS relativistic calculations, despite the inherent simplicity of the algorithm, are highly demanding in terms of computer resources as a consequence of the explicit manipulation of four-component complex vectors. Calculations were, therefore, run on a Vax 8800 computer.

Results and Discussion

The MCp_3 Fragment. The present alkoxide derivatives possess a distorted pseudotetrahedral ligation arrangement (Chart I). The bonding of f-element metals in the Cp_3M (C_{3v} symmetry) cluster has been analyzed previously.[1,3] It involves MOs which, depending upon their energy, are combinations of ligand Cp π_2 MOs[18] and f and/or d metal orbitals.[3] Their energies have been found[3] to lie in the sequence

$$a_2 > e(2) \approx a_1 > e(1)$$

The nonlinear arrangement along the M–O–R bond vector lowers

(14) Casarin, M.; Vittadini, A.; Granozzi, G.; Fragalà, I.; Di Bella, S. *Chem. Phys. Lett.* **1987**, *141*, 193–197.
(15) Slater, J. C. *Quantum Theory of Molecules and Solids. The Self-Consistent Field for Molecules and Solids*; McGraw-Hill: New York, 1974; Vol. 4.
(16) (a) Ellis, D. E.; Rosen, A.; Gubanov, V. A. *J. Chem. Phys.* **1982**, *77*, 4051–4060. (b) Koelling, D. D.; Ellis, D. E.; Bartlett, R. J. *J. Chem. Phys.* **1976**, *65*, 3331–3340. (c) Rosen, A.; Ellis, D. E. *J. Chem. Phys.* **1975**, *62*, 3039–3049. (d) $p = -ihD$ is the usual momentum operator; α and β are the velocity operators

$$\alpha = \begin{vmatrix} 0 & \sigma \\ \sigma & 0 \end{vmatrix} \quad \text{and} \quad \beta = \begin{vmatrix} I & 0 \\ 0 & I \end{vmatrix}$$

where σ represent the 2 × 2 Pauli spin matrices (σ_x, σ_y, σ_z) and I is the 2 × 2 unit matrix.
(17) (a) Raymond, K. N. In *Organometallics of the f-Elements*; Marks, T. J., Fischer, R. D., Eds.; Reidel Publishing Co.: Dordrecht, Holland, 1979; pp 249–280. (b) Marks, T. J. *Prog. Inorg. Chem.* **1979**, *25*, 224–333 and references therein.
(18) (a) Evans, S.; Green, M. L. H.; Jewitt, B.; Orchard, A. F.; Pygall, C. F. *J. Chem. Soc., Faraday Trans. 2* **1972**, 1847–1865. (b) Evans, S.; Green, M. L. H.; Jewitt, B.; King, G. H.; Orchard, A. F.; Pygall, C. F. *J. Chem. Soc., Faraday Trans. 2* **1973**, 356–376.

Table I. Eigenvalues and Population Analysis of Selected Higher Lying Orbitals for Cp_3CeOCH_3 (C_s Symmetry)

MO	−eV GS	eV TSIE	eV IE[a]	Ce 6s	Ce 6p	Ce 5d	Ce 4f	3Cp	O	CH_3	character
27a′	4.17			0	0	0	97	2	1	0	$f_{z(x^2-y^2)}$ (LUMO)
20a″	5.20	7.31	7.37 (**a**)	0	0	2	25	66	6	1	$\pi_2 + f_{yz^2}$ (HOMO)
26a′	5.32	7.32		0	1	0	6	83	8	2	π_2
19a″	5.40	7.43	7.81 (**b**)	0	0	0	21	79	0	0	$\pi_2 + f_{y(3x^2-y^2)}$
25a′	5.38	7.49		0	0	2	15	77	5	1	$\pi_2 + f_{xz^2}$
18a″	6.13	8.26	8.56 (**c**)	0	0	5	4	62	23	6	π_2 + O 2p
24a′	6.37	8.59		0	0	4	3	42	42	9	O 2p + π_2
17a″	6.57	8.81	9.41 (**d**)	0	0	10	3	39	39	9	O 2p + π_2 + d_{yz}
23a′	6.67	8.92		0	0	7	2	69	18	4	π_2 + O 2p + d_{xz}
15a′	10.58			0	0	6	2	7	63	22	σ Ce–O

[a] Letters in parentheses refer to PES features in Figure 5.

Table II. Eigenvalues and Population Analysis of Selected Higher Lying Orbitals for Cp_3ThOCH_3 (C_s symmetry)

A. C_s Symmetry

MO	−eV GS	eV TSIE	eV IE[a]	Th 7s	Th 7p	Th 6d	Th 5f	3Cp	O	CH_3	character
27a′	3.14			0	0	3	88	9	0	0	$f_{z(x^2-y^2)}$ (LUMO)
26a′	5.35	7.49	7.63 (**a**)	0	0	0	5	77	15	3	$\pi_2 + f_{xz^2}$ (HOMO)
20a″	5.36	7.52		0	0	1	14	65	16	4	$\pi_2 + f_{yz^2}$
19a″	5.51	7.75	8.15 (**b**)	0	0	1	10	89	0	0	$\pi_2 + f_{y(3x^2-y^2)}$
25a′	5.61	7.84		0	0	2	2	86	8	2	π_2
18a″	6.24	8.46	8.84 (**c**)	0	0	6	2	54	32	8	O 2p + π_2
24a′	6.41	8.70		0	0	5	2	49	35	9	O 2p + π_2
17a″	6.86	9.57	10.05 (**d**)	0	0	13	1	60	20	6	π_2 + O 2p + d_{yz}
23a′	6.94	10.11		0	0	9	1	71	15	4	π_2 + O 2p + d_{xz}
15a′	10.73			0	0	5	2	12	59	22	σ Th–O

B. C_{3v} Symmetry

MO	GS, −eV	TSIE, eV	Th 7s	Th 7p	Th 6d	Th 5f	3Cp	O	CH_3	character
$5a_2$	5.30	7.54	0	0	0	11	89	0	0	π_2 + f
15e	5.55	7.70	0	0	0	13	62	20	5	π_2 + O 2p + f
$11a_1$	5.69	7.92	0	0	0	2	94	3	1	π_2
14e	6.09	8.35	0	0	4	1	71	19	5	π_2 + O 2p
13e	6.75	9.69	0	0	12	1	49	29	9	O 2p + π_2 + d
$7a_1$	10.52		0	0	7	2	30	45	16	σ Th–O

Table III. Eigenvalues and Population Analysis of Selected Higher Lying Orbitals for Cp_3UOCH_3 (C_s Symmetry)

MO	−eV GS	eV TSIE	eV IE[a]	U 7s	U 7p	U 6d	U 5f	3Cp	O	CH_3	character
21a″	3.85			0	0	2	93	4	1	0	f_{xyz} (LUMO)
27a′	3.87	6.29	6.55 (**x**)	0	0	1	93	5	1	0	$f_{z(x^2-y^2)}$ (HOMO)
26a′	5.35	7.44	7.74 (**a**)	0	0	0	3	90	5	2	π_2
20a″	5.36	7.46		0	0	2	23	67	7	1	$\pi_2 + f_{yz^2}$
19a″	5.54	7.61	8.35 (**b**)	0	0	0	18	82	0	0	$\pi_2 + f_{y(3x^2-y^2)}$
25a′	5.58	7.67		0	0	2	18	71	7	2	$\pi_2 + f_{xz^2}$
18a″	6.16	8.31	8.99 (**c**)	0	0	5	4	55	29	7	π_2 + O 2p
24a′	6.34	8.40		0	0	3	3	62	30	2	π_2 + O 2p
17a″	6.68	9.41	10.13 (**d**)	0	0	10	2	48	32	8	O 2p + π_2 + d_{yz}
23a′	6.74	9.42		0	0	7	3	58	26	6	O 2p + π_2 + d_{xz}
15a′	10.71			0	0	4	2	10	62	22	σ U–O

[a] Letters in parentheses refer to PES features in Figure 6.

the symmetry to C_s, thus lifting the degeneracy of MOs of e symmetry (e = a′ + a″), and might, in principle, alter the above orbital sequence as well.[1a] It will be seen that these effects are rather small (vide infra).

The $-OCH_3$ Fragment. Within a localized bonding model,[19] the $-OCH_3$ ligand possesses, in addition to methyl orbitals, three O 2p lone pair orbitals,[8,9a,20] one of which remains collinear with the C–O axis and transforms as a_1 in C_{3v} symmetry. The remainder form a 2-fold degenerate set of e symmetry. In a linear M–O–C conformation, the a_1 MO will be involved in the formation of the M–O σ bond and will be lower[8,9a] lying relative to the e MOs which, in turn, formally represent a π symmetry set. We shall be mainly concerned with the latter π set which is expected to lie in the same energy range as Cp π_2-based MOs.[8] By symmetry, the π set can interact with p, d, and f metal basis orbitals. Qualitatively, donation into empty metal orbitals results in the stabilization of these π O 2p lone pairs which, therefore, provide a nonnegligible contribution to the M–O bond. Upon bending of the M–O–C vector from collinearity, the O 2p orbital, normal to the plane defined by the M–O–C linkages, remains purely π in character whereas the O 2p orbital, lying in the plane, rehybridizes to σ sp^2 character by mixing with both σ O–C and $-CH_3$ bonds of suitable symmetry. An obvious consequence of

(19) Cox, P. A.; Evans, S.; Orchard, A. F.; Richardson, N. V.; Roberts, P. J. *J. Chem. Soc., Faraday Discuss.* **1972**, *54*, 26–40.

(20) (a) Kober, E. M.; Lichtenberger, D. L. *J. Am. Chem. Soc.* **1985**, *107*, 7199–7201. (b) Bursten, B. E.; Cotton, F. A.; Green, J. C.; Seddon, E. A.; Stanley G. G. *J. Am. Chem. Soc.* **1980**, *102*, 4579–4588. (c) Kimura, K.; Katsumata, S.; Achiba, Y.; Yamazaki, T.; Iwata, S. *Handbook of HeI Photoelectron Spectra of Fundamental Organic Molecules*; Japan Scientific Societies Press: Tokyo, 1981.

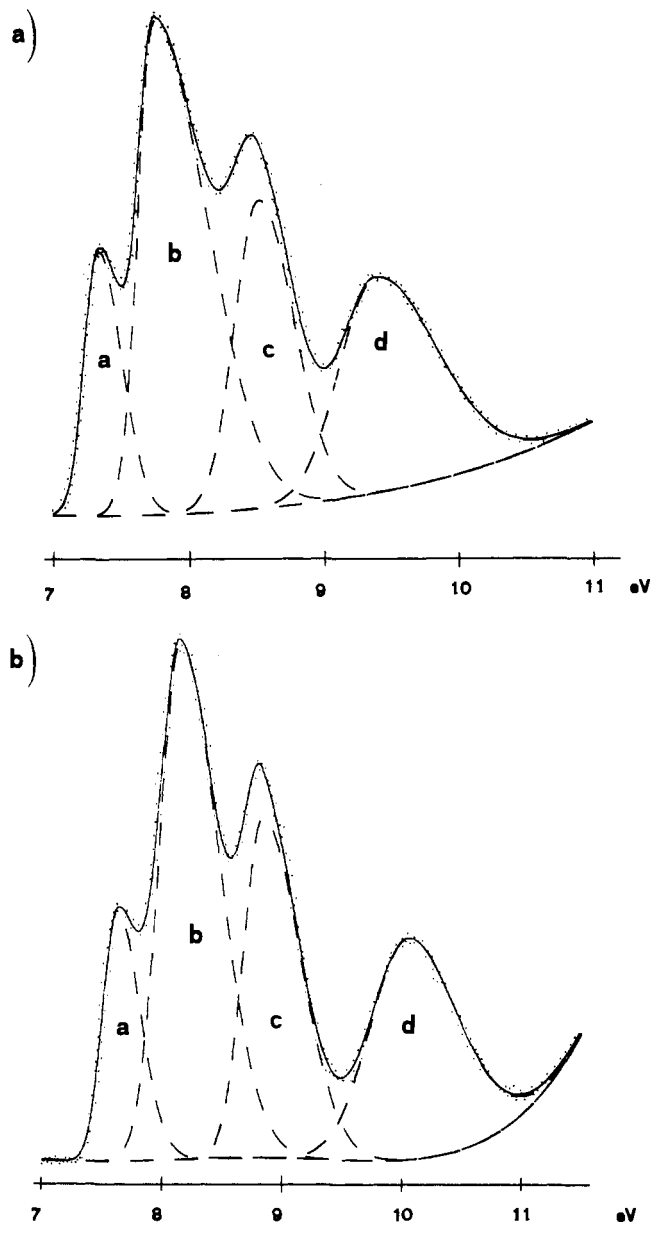

Figure 5. He I photoelectron spectra of (a) $Cp_3Ce(O\text{-}i\text{-}Pr)$ (6.9–11.3 eV) and (b) Cp_3ThOCH_3 (6.9–11.6 eV).

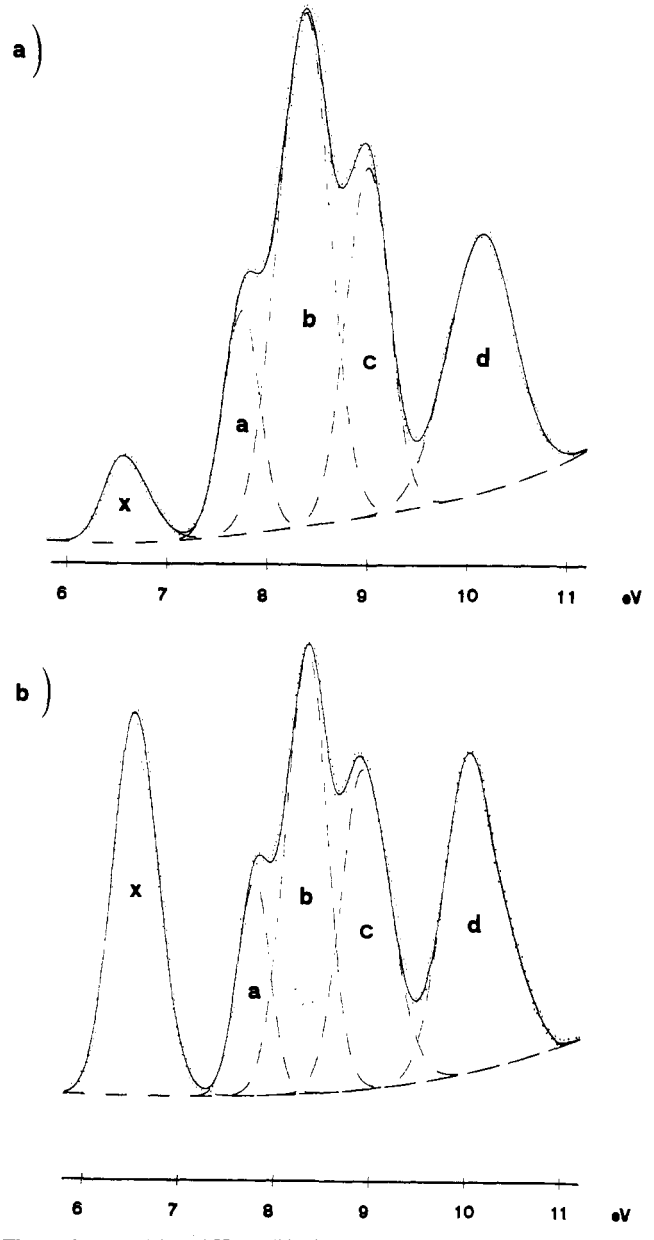

Figure 6. He I (a) and He II (b) photoelectron spectra of $Cp_3UOC_2H_5$ (5.8–11.2 eV).

these interactions with lower lying σ orbitals is a significant energetic destabilization.

Theoretical Results. Tables I–III present the nonrelativistic Xα results for the present Cp_3MOR complexes. Because of the low symmetry, the MOs are heavily admixed; however dominant orbital characters are easily recognized. In the case of M = U, the HOMO, 27a′, consists of an almost totally metal-based MO which is nearly degenerate with the 21a″ LUMO. The corresponding 27a′ MOs are clearly the LUMOs when M = Th or Ce. The major source of the metal–Cp bonding is invariably provided by the 20a″ MO and involves the metal $5f_{yz^2}$ AO. This AO (Figure 1), as found in earlier studies,[1a,2a,b] is ideally suited for stabilizing the Cp_3 template. The 19a″ MO provides a significant contribution as well. Both of these MOs are dominated by 5f/4f interactions which are similar for M = U and Ce and somewhat diminished for M = Th. Several lower energy MOs comprise the M–O π bonding orbitals and possess both O 2p π and relevant metal d character. Concurrent admixtures with Cp π_2 and with MOs representing methyl C–H bonds are also found and indicate interligand interactions. A contour plot analysis (Figure 2) unequivocally shows large π M–O bonding interactions as well as the involvement of primarily 6d-based metal AOs. Interestingly, sizable O 2p admixtures (more important in the M = Th complex) are found even in the 26a′ and 20a″ MOs. In sum, several MOs are found to contribute to the substantial M–O π bonding, and this result agrees well with the short[21] M–O bond lengths and large M–O–C angles found diffractometrically in early transition and f-element complexes,[9a,21] as well as with electric dipole moment results on Cp_3UOR complexes.[22] The lower energy 15a′ MO represents a purely σ bonding MO.

Upon linearization of the Th–O–CH_3 vector under the more symmetric C_{3v} geometry, similar results are obtained as far as the

(21) (a) Van Der Sluys, W. G.; Sattelberger, A. P. *Chem. Rev.* **1990**, *90*, 1027–1040. (b) Caulton, K. G.; Hubert-Pfalzgraf, L. G. *Chem. Rev.* **1990**, *90*, 969–995. (c) Cayton, R. H.; Chisholm, M. H.; Clark, D. L.; Hammond, C. E. *J. Am. Chem. Soc.* **1989**, *111*, 2751–2755. (d) Ziegler, T.; Tschinke, V.; Versluis, L.; Baerends, E. J.; Ravenek, W. *Polyhedron* **1988**, *7*, 1625–1637. (e) Blake, P. C.; Lappert, M. F.; Taylor, R. G.; Atwood, J. L.; Zhang, H. *Inorg. Chim. Acta* **1987**, *139*, 13–20. (f) Cotton, F. A.; Marler, D. O.; Schwotzer, W. *Inorg. Chim. Acta* **1984**, *95*, 207–209. (g) Cotton, F. A.; Marler, D. O.; Schwotzer, W. *Inorg. Chim. Acta* **1984**, *85*, L31–32. (h) Duttera, M. R.; Day, V. W.; Marks, T. J. *J. Am. Chem. Soc.* **1984**, *106*, 2907–2912. (i) Marks, T. J.; Manriquez J. M.; Fagan, P. J.; Day, V. W.; Day, C. S.; Vollmer, S. H. *ACS Symp. Ser.* **1980**, *131*, 1–29. (j) Bradley, D. C.; Mehrotra, R. C.; Gaur, D. P. *Metal Alkoxides*; Academic Press: New York, 1978. (k) Bradley, D. C. *Adv. Inorg. Chem. Radiochem.* **1972**, *15*, 259–322. (l) Bradley, D. C.; Fisher, K. *J. MTP Int. Rev. Sci.: Inorg. Chem., Ser. One* **1972**, *5*, 65–78

(22) Fischer, R. D. In in ref 1d, pp 277–326.

Table IV. Relativistic Eigenvalues and Population Analysis of Selected Higher Lying Orbitals for Cp_3ThOCH_3 (C_{3v} Symmetry)

		Th										
MO	GS, –eV	$6s_{1/2}$	$6p_{1/2}$	$6p_{3/2}$	$d_{3/2}$	$d_{5/2}$	$f_{5/2}$	$f_{7/2}$	$7s_{1/2}$	3Cp	O	CH_3	character
$35e_{1/2}$	2.58	0	0	0	7	2	54	16	0	21	0	0	f + π_2 (LUMO)
$34e_{1/2}$	5.54	0	0	0	0	0	5	6	0	89	0	0	π_2 + f (HOMO)
$16e_{3/2}$	5.55	/	/	0	0	0	6	8	/	37	44	5	O 2p + π_2 + f
$33e_{1/2}$	5.57	0	0	0	0	0	8	6	0	40	41	5	O 2p + π_2 + f
$32e_{1/2}$	5.88	0	0	2	1	1	0	1	0	93	1	1	π_2
$15e_{3/2}$	6.25	/	/	1	5	6	1	0	/	70	15	2	π_2 + d
$31e_{1/2}$	6.40	0	0	0	2	9	0	1	0	70	16	2	π_2 + d
$14e_{3/2}$	6.97	/	/	0	9	11	0	0	/	65	13	2	π_2 + d
$30e_{1/2}$	6.98	0	0	0	9	12	0	0	0	62	14	3	π_2 + d
$19e_{1/2}$	11.20	0	1	4	3	5	1	2	2	15	45	22	σ Th–O

Table V. Photoelectron Spectroscopic Data for Cp_3MOR Complexes, Including Line Widths and Related Band Intensities

band		He I			He II		
label	IE,[a] eV	W_L	W_R	rel int[b]	W_L	W_R	rel int[b]
			$Cp_3Ce(O\text{-}i\text{-}Pr)$				
a	7.37	0.28	0.37	0.88	0.33	0.38	0.89
b	7.81	0.41	0.81	3.11	0.45	0.82	3.06
c	8.56	0.43	0.57	1.78	0.43	0.60	1.80
d	9.41	0.65	1.06	2.21	0.65	1.08	2.24
			Cp_3ThOCH_3				
a	7.63	0.28	0.45	0.87	0.30	0.46	0.88
b	8.15	0.40	0.75	2.93	0.40	0.75	2.89
c	8.84	0.38	0.73	1.97	0.39	0.73	1.99
d	10.05	0.73	1.00	2.22	0.73	1.01	2.20
			$Cp_3UOC_2H_5$				
x	6.55	0.45	0.60	0.40	0.50	0.61	2.40
a	7.74	0.42	0.44	0.91	0.43	0.44	0.92
b	8.35	0.59	0.60	3.02	0.61	0.62	2.50
c	8.99	0.50	0.51	1.81	0.50	0.71	1.95
d	10.13	0.76	0.78	2.27	0.76	0.79	2.63

[a] IEs are related to the position of the Gaussian components. [b] Relative intensities of bands **a**–**d** are normalized to the total intensity of low-energy bands assumed equal to 8.0.

MO sequences and groupings are concerned (Table II). Of course, the classical sequence $a_2 > e \approx a_1 > e$, nearly ubiquitous in C_{3v} Cp_3ML complexes,[3,8] is observed in the case of Cp π_2-related MOs. Moreover, no significant changes are observed in the atomic composition of various MOs, thus reflecting similar metal–ligand interactions in both linear and bent geometries.

Table IV sets out the fully relativistic DS Xα–DVM results for Cp_3ThOCH_3. Symmetry labels, of course, refer to the double-spinor C_{3v}^* group since the Hamiltonian explicitly includes spin–orbit coupling.[16] Correspondences among representations of pertinent point groups are as follows:

C_s	C_{3v}	C_{3v}^*	Bethe notation
a′	a_1	$e_{1/2}$	Γ_4
a″	a_2	$e_{1/2}$	Γ_4
a′ + a″	e	$e_{1/2} + e_{3/2}$	$\Gamma_4 + (\Gamma_5 + \Gamma_6)$

In Figure 3, relativistic results for C_{3v} Cp_3ThOCH_3 are compared with the nonrelativistic results for the linear (C_{3v}) and bent (C_s) Th–O–CH_3 conformations. Correlations among various orbitals are made by reference to the dominant metal content. Similar to the nonrelativistic results, relativistic metal–ligand interactions represented by more external MOs primarily involve metal 5f AOs. Lower lying orbitals, in contrast, are only metal 6d admixed. The total extent of metal participation found in the uppermost filled MOs is comparable in both relativistic and nonrelativistic cases (9 vs 13%). The 5f contribution remains nearly constant (4.6 vs 5%) while the amount of 6d participation is significantly increased in the DS results (4.6 vs 8%). The LUMO remains mostly metal 5f in character (70 vs 88%) while the $19e_{1/2}$ MO, responsible for the M–O σ bond, is clearly dominated by interactions with metal $6d_{z^2}$ (8%) and, to a lesser extent, with 5f (3%) AOs. These results are entirely consistent with Xα–SW results on the UCp_3OH model structure reported by Bursten,[3a] once the quasi-relativistic nature and the neglect of the methyl group in the latter calculations are taken into account.

It is a generally held view that s and p orbitals of heavy elements are contracted under the influence of relativistic effects while d and f orbitals expand, because of a major shielding of the nuclear charge.[23] In the present case, the relativistic 6d populations found for various Cp_3ThOCH_3 MOs follow the expected trend while the nearly constant 5f admixture in both relativistic and nonrelativistic calculations represents a counterintuitive finding. Nevertheless, an important change in the energy spectrum of virtual orbitals upon changing to the relativistic regime is the destabilization of both atomic f and d orbitals.[23] A differential effect, however, causes a larger shift of 5f orbitals, and hence, the 5f and 6d orbitals move closer together in energy.[23a] This effect can be seen in the results of parallel calculations on the bare metal ions reported in Figure 4. Obvious consequences are less favorable relativistic energy denominators which, in the case of 5f subshells, counterbalance better metal–ligand overlaps. The net result is an almost constant 5f admixture in both relativistic and nonrelativistic cases. In addition, the $16e_{3/2}$ and $33e_{1/2}$ MOs have increased O 2p contributions relative to corresponding nonrelativistic eigenvectors (Tables II and IV). This finding may be associated with relativistically more expanded metal AOs which favor extensive metal-mediated interligand mixing.

Photoelectron Spectra. The lower energy features of the present PE spectra (Figures 5 and 6) are similar to those found in several Cp_3MX spectra reported previously.[1a] The spectra all consist of well-resolved triplet features (labeled **a**–**c** in the figures) having 1:3:2 intensity ratios and of a fully resolved band **d** in the 9.40–10.14-eV range. Nonrelativistic DV–Xα TSIEs provide an accurate fitting of IE values as well as of the band grouping (Tables I–III). Even though relativistic TSIE values of Cp_3ThOR have not been evaluated, the close coincidence of GS eigenvalues with the nonrelativistic results (Tables IIA and IV) is clearly indicative of an insignificant improvement in accuracy on passing to DS calculations. Furthermore, it is noted that the band groupings are somewhat better reproduced by the nonrelativistic calculations on the fully symmetrized C_{3v} structure (Table IIB, Figure 5). This observation together with the absence of any additional structure associated with all of the PE bands raises the possibility of some expansion of the M–O–CH_3 angle in the gas phase.

The assignment of PE spectra is, therefore, a straightforward matter (Tables I, IIA and III). Bands **a**–**c** represent ionizations of MOs mostly related to the π_2 Cp combination (Figures 5 and 6). Band **d** can be assigned to MOs which nominally are O 2p lone pairs. Note that the greater Cp–L interligand admixture renders, in most cases, any classification in accordance with a dominant atom character purely nominal.

(23) (a) Boerrigter, P. M.; Baerends, E. J.; Snijders, J. G. *Chem. Phys.* **1988**, *122*, 357–374. (b) Höhl, D.; Ellis, D. E.; Rösch, N. *Inorg. Chim. Acta* **1987**, *127*, 195–202. (c) Ziegler, T.; Snijders, J. G.; Baerends, E. J. *J. Chem. Phys.* **1981**, *74*, 1271–1284.

Table VI

Electronic Charges and Overlap Populations for Cp_3MOCH_3 Complexes

	charge, eu							
	M							
complex	f	d	s	p		Cp	$-OCH_3$	overlap pop.
$CeCp_3OCH_3$	1.56	0.75	0.03	0.07	+1.59	−0.465	−0.195	Ce- -Cp = 0.125 Ce- -O = 0.853
UCp_3OCH_3	3.40	0.71	0.02	0.06	+1.815	−0.518	−0.261	U- -Cp = 0.050 U- -O = 0.709
$ThCp_3OCH_3$	0.89	0.92	0.02	0.06	+2.105	−0.590	−0.335	Th- -Cp = 0.104 Th- -O = 0.740

Relativistic Data for Cp_3ThOCH_3

charge, eu										
Th (+2.250)										
$5f_{5/2}$	$5f_{7/2}$	$6s_{1/2}$	$6p_{1/2}$	$6p_{3/2}$	$6d_{3/2}$	$6d_{5/2}$	$7s_{1/2}$	Cp	$-OCH_3$	overlap pop.
0.355	0.362	1.964	1.942	3.781	0.561	0.709	0.069	−0.635	−0.341	Th- -Cp = 0.180 Th- -O = 0.602

The IE values associated with various bands are closely comparable in the U and Th spectra with an almost constant spectral width (≈2.45 eV; Figures 5b and 6). In the Ce complex (Figure 5a), a narrower total width (≈2.0 eV), as well as a different energy spacing among various bands, is observed. The same trend is accurately reproduced by the theoretical calculations in terms of the upward–downward shifts of the 18a″ and 23a′ MOs due to smaller interactions involving the intermediate-energy 24a′ and 17a″ MOs.

The spectra of the M = U complex (Figure 6) show the usual onset feature (labeled x in the figure), which is lacking in the $4f^0$ and $5f^0$ homologues and which undergoes the classical He II intensity enhancement, always associated[1a,c,24] with the production of the $^2F_{5/2}$ ion state from the $^3H_4$ U(IV) $5f^2$ configuration. The remaining low-IE features do not undergo sizable changes of relative intensities upon switching to He II radiation when M = Th and Ce (Table V). The He II spectrum of the M = U complex (Figure 6) exhibits a different pattern since band **d** appears somewhat increased in relative intensity (Table V). The observed trend is in agreement with the atomic compositions of corresponding MOs.[25]

Concluding Remarks

The electronic structure of a series of homologous 4f and 5f Cp_3MOR alkoxide complexes has been studied using SCF Xα–DVM calculations. Fully relativistic DS calculations have been also performed for the M = Th complex. Comparison of the calculations reveals that metal d contributions are somewhat underestimated in the nonrelativistic description even though deviations do not alter the overall description of the metal–ligand bonding. Metal–ligand bonding (M–OR) involves two-orbital two-electron interactions and causes ligand → metal charge transfer resulting in the U $5f^{3.40}6d^{0.71}$ and Ce $4f^{1.56}5d^{0.75}$ configurations (Table VI). It is noteworthy that the uranium electron configuration is very close to that found both in previously studied Cp_3UX analogues[1a] ($5f^{3.4}6d^{0.7}$) and with fully relativistic SCF–DS calculations on the uranium atom.[23a] In the case of the M = Th complex (Table V), the nonrelativistic configuration Th $5f^{0.89}6d^{0.92}7s^{0.02}7p^{0.06}$ compares well with relativistic result of $5f^{0.72}6d^{1.27}6s^{1.96}6p^{5.72}7s^{0.07}$ with differences being similar to that found in earlier studies.[23b,7] The total metal–ligand covalency, however, remains almost constant with a +2.25 metal charge (+2.105 nonrelativistically). The maximum covalency within the series is found in Cp_3CeOCH_3 with 2.41 electrons transferred to the metal center. The M = U complex (Table V) follows with 2.185 and then the M = Th complex with 1.895. This trend parallels the findings of relativistic ab initio and quasi-relativistic SCF–Xα–SW results for $M(\eta^8\text{-}C_8H_8)_2$ (M = Th, U, Ce) complexes.[7]

The M–O bonding in Cp_3MOCH_3 complexes has both σ and π character and involves charge transfer along the $CH_3 \rightarrow O \rightarrow M \rightarrow Cp_3$ direction. As found in $U(OCH_3)_6$,[9a] U–O π bonding provides a satisfactory explanation for the shorter U–O distance as well as for the strong propensity to maintain almost linear U–O–CH_3 linkages.[21] It is likely that the involvement of the methoxide methyl group in the U–O π bonding[21] contributes to these trends.

Finally we comment on costs and benefits associated with the use of the fully relativistic local density Dirac–Slater formalism for molecular calculations. At present, the extensive use of such calculations is not practicable because of the necessary computational demands. Such calculations do, however, provide a more accurate description of the metal–ligand bonding, thus better defining the relative roles of metal 6d and 5f covalency. Furthermore, the more appropriate evaluation of the radial and angular expansion of the metal subshells is useful for a more accurate description of the π donor properties of ligands such as the alkoxy ligand, thus better explaining the geometries adopted in f-element alkoxide complexes.[9a,21] It is worthwhile to emphasize here that the general chemical description of the bonding in the present complexes does not change greatly from the nonrelativistic to relativistic treatment as far as interpretation of PE spectra is concerned. Note that IE values can be accurately and comparably evaluated at the nonrelativistic level once optimized basis sets and potential representation are used. No significant improvement is expected in TSIE values at the DS level since GS eigenvalues are comparable in both cases while reorganization effects must be similar at both levels.

Acknowledgment. The authors gratefully thank the Ministero della Ricerca Scientifica e Tecnologica "MURST" (I.F.) and the U.S. National Science Foundation (T.J.M., Grant CHE 9104112) for financial support.

(24) (a) Brennan, J. G.; Green, J. C.; Redfern, C. M. *J. Am. Chem. Soc.* **1989**, *111*, 2373–2377. (b) Egdelll, R. G. Ph.D. Thesis, Oxford, 1977. (c) McLaughlin, R. *J. Chem. Phys.* **1962**, *36*, 2699.

(25) Rabelais, J. W. *Principles of UV Photoelectron Spectroscopy*; J. Wiley & Sons: New York, 1977.